Chapter 6
An Empirical Assessment of Variable Water Content and Grain-Size on X-Ray Fluorescence Core-Scanning Measurements of Deep Sea Sediments

Suzanne E. MacLachlan, James E. Hunt and Ian W. Croudace

Abstract Deciphering the signal within X-ray fluorescence (XRF) core scanner data can be complex in comparison to conventional laboratory XRF analysis where samples are milled and pelleted or beaded. One complicating factor is that the down-core variability in water content and grain-size can affect element count rates thereby potentially leading to inaccurate interpretations. Experiences using an Itrax XRF core scanner data highlight some of the pitfalls that can occur when the sediment is inhomogeneous. We show that over a threshold of 25 wt.% coarse grained material (>63 μm) within the sediment there is a potential for causing significant variability in certain elements. It is also shown that water content variability has a major effect above 40 %.

Keywords X-ray fluorescence · XRF core scanner · Water content · Physical properties · Marine sediment

S. E. MacLachlan (✉)
National Oceanography Centre, European Way, Southampton SO14 3ZH, UK
e-mail: s.maclachlan@noc.ac.uk

J. E. Hunt
Marine Geoscience, National Oceanography Centre, European Way,
Southampton SO14 3ZH, UK

I. W. Croudace
Ocean and Earth Science, National Oceanography Centre, University of Southampton,
Waterfront Campus, European Way, Southampton SO14 3ZH, UK

I. W. Croudace, R. G. Rothwell (eds.), *Micro-XRF Studies of Sediment Cores*,
Developments in Paleoenvironmental Research 17, DOI 10.1007/978-94-017-9849-5_6

Introduction

Micro X-ray fluorescence (XRF) core scanners are now widely used in sediment core research. These core scanners are employed as a rapid analytical tool in palaeoceanography (e.g. Ziegler et al. 2013), palaeoliminology (e.g. Guyard et al. 2007), geochemical investigations (e.g. Tian et al. 2011) and geochronological studies (e.g. Rothwell et al. 2006; Westerhold et al. 2007; Hunt et al. 2013). A major advantage of these core scanners, compared to conventional laboratory XRF analysis, is the rapid acquisition of high resolution continuous down-core elemental data without disturbance to the split sediment core. However, interpretation of XRF core scanner data can be more complex than conventional lab WD-XRF (wavelength dispersive x-ray fluorescence spectrometry) analysis, because of the range of variables that exist when analysing the surface of a split sediment core. For instance, even when carefully cut, split cores may have an uneven surface topography and grain-size variations will result in surface roughness (Rothwell and Rack 2006). Other data inaccuracies may occur due to variable interstitial water content, sediment surface mineral homogeneity, textural and porosity variability, and potential pooling of water between the sediment surface and x-ray film driven by capillary flow (Tjallingii et al. 2007).

Over the past decade efforts have been made to evaluate the accuracy and precision of XRF core scanners, addressing issues related to sediment surface heterogeneity (e.g. Richter et al. 2006; Tjallingii et al. 2007; Hennekam and de Lange 2012; Wilhelms-Dick et al. 2012). However, the majority of the published work relates to investigations using the Avaatech core scanner, and only limited consideration has been given to sediment cores run using the widely used Itrax core scanner.

The designs of the Itrax and Avaatech scanners are different, perhaps leading to slightly different data acquisition capabilities. The Avaatech scanner utilises a prism system that is lowered onto the sediment surface at each measurement point, and incoming radiation strikes the sample surface at 45°. The detector for outgoing fluorescent x-rays is likewise mounted at an angle of 45° (Richter et al. 2006). The Itrax core scanner has an incident radiation beam that is 90° to the sample surface. Samples are initially topographically scanned to generate a smoothed distance profile that is used to guide the position of a moveable XRF detector. The XRF detector therefore should remain at a constant distance to the sample surface as the sediment core is incrementally moved (Croudace et al. 2006).

Here, we review the effects of heterogeneity of the sediment surface, specifically examining variable water content and grain-size within a marine sediment core using an Itrax core scanner. The results are compared to published studies obtained with an Avaatech core scanner system. This contribution examines the impact of sediment surface heterogeneities on XRF elemental signals.

Materials and Methods

Sediment Material

Sediment core JC060-021-PC05 is a 667 cm-long core that was recovered from a water depth of 1054 m during the RRS James Cook cruise JC060 to the eastern mound field of the Darwin mounds area (59°50.882'N, 7°3.659'W) in the northern Rockall Trough, northwest of the UK (Fig. 6.1). The sediment input to the northern Rockall Trough has been minimal since the last glaciation. The Holocene sedimentary regime has been controlled by strong bottom currents redistributing older sediments (Kenyon 1986; Stoker et al. 1998; Masson et al. 2002, 2003). Regionally, the upper few metres of sediment on the lower slopes and basin floor of the northern Rockall Trough typically consist of a thin (<20 cm) surface layer of coarse, sandy Holocene sediment overlying thick glaciogenic mud containing sparse coarse-

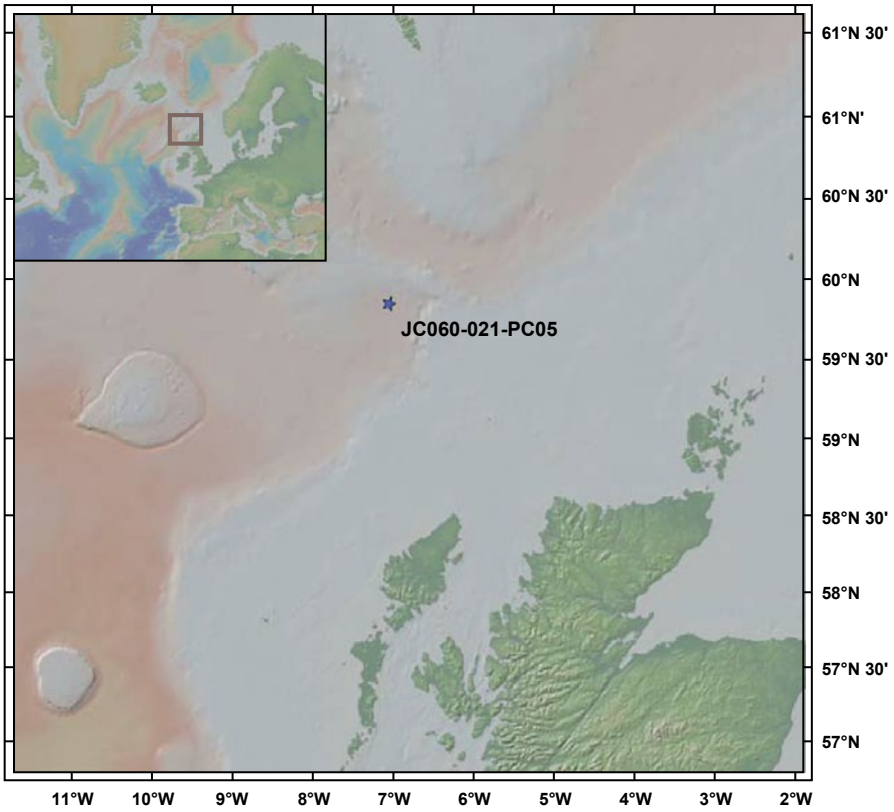

Fig. 6.1 Location of core JC060-021-PC05 and the regional setting of the Darwin mounds area in the northern Rockall Trough, northwest Scotland. The base map is from the Global Multi-Resolution Topography (GMRT) synthesis. (Ryan et al. 2009)

grained horizons (Howe 1995, 1996). The core was selected for this study as it was not split at sea, thus allowing whole core logging of the physical properties and minimal loss of water content prior to analysis.

XRF-Core Scanning

XRF measurements were obtained directly from the split core surface of the archive half with the Itrax XRF core scanner at the British Ocean Sediment Core Research Facility at National Oceanography Centre, Southampton (UK). XRF data were acquired using a molybdenum X-ray tube set at 30 kV and 50 mA with a dwell time of 30 s and a step size of 1 mm. The Itrax X-ray beam (0.2×20 mm) is used to irradiate (excite) samples to generate a radiographic image and an energy-dispersive X-ray spectrum. This spectrum is derived from a somewhat smaller area than the full 20 mm beam width and is determined (especially so for lighter elements) by the 5 mm diameter vacuum nozzle connected to the SDD detector. The sample can remain statically in the beam for the chosen dwell time in which case the spectrum accumulated relates to an area of $0.2 \times \sim 5$ mm. Alternatively, the user can select a dynamic scan where the core moves through the Itrax beam according to the selected scan distance and dwell time.

The dataset from the Itrax core scanner is different from conventional laboratory XRF measurements where individual samples (typically 0.5 or 1 cm sub-samples cut out of the core) are measured in a vacuum as either homogeneous compact pellets or beads having a flat surface. The Itrax generates a single dispersive energy spectrum for each point down core, and each element intensity is calculated as a peak area (expressed in counts). The counts are not normally matrix corrected and several previous studies have shown that there is a good first approximation to concentration (e.g. Croudace et al. 2006, 2015, this volume). Users also commonly take small subsamples and analyse using a quantitative destructive method (ICP-OES or WD-XRF) to validate/calibrate Itrax data. In this study the Itrax data are directly compared with elemental concentrations derived using WD-XRF. The Itrax-scan data (1 mm resolution) have been averaged over 10 points to allow comparison with the WD-XRF data (1 cm resolution, the method used by Hunt et al. 2015, this volume).

Conventional WD-XRF

Twenty-six 1 cm resolution subsamples were selected from a range of water contents (20.0–40.2 %; see Fig. 6.2 and Sect. 2.6) within the sediment core for conventional WD-XRF analysis. WD-XRF subsamples were selected to encompass the variability observed in the physical properties down-core. Subsamples were pressed into pellets and analyzed using a Philips Magix-Pro instrument fitted with a 4 kW Rh-target X-ray tube. The instrument was calibrated using a range of international geochemical reference samples with matrix correction applied using Compton correction and fundamental parameters models.

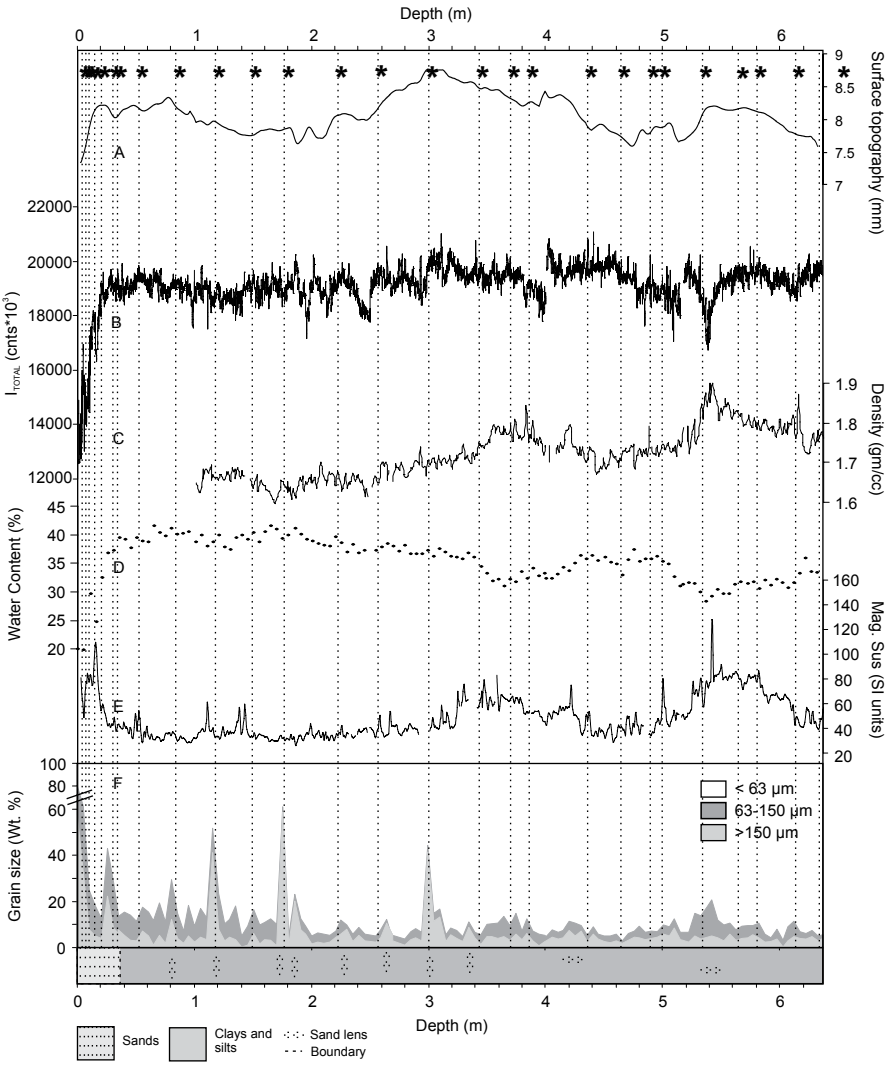

Fig. 6.2 Compilation of parameters measured on sediment core: **a** surface topography from the Itrax; **b** total counts from the Itrax; **c** density from the MSCL-S; **d** percentage water content; **e** magnetic susceptibility measured on MSCL-XYZ; **f** variability of the grain-size fractions < 63 µm, 63–150 µm, and > 150 µm, in weight %. At the base of the compilation of parameters is the lithological log and key. The *asterisk* (*) and *dotted lines* indicate the locations of WD-XRF subsamples

Grain-Size

Sediment core JC60-21 was sampled at 5 cm intervals for laser diffraction grain-size analysis. No pre-treatment was considered necessary due to previous studies indicating low total organic carbon values (typically 0.02 %, Serpetti et al.

2013). Subsamples were dispersed in 30 mL of RO water with 0.05% sodium hexametaphosphate dispersant and left on a shaking table for 12 h. The dispersed sediment solutions were analysed using a Malvern (model *Mastersizer 2000*) particle size analyser, which is able to measure grain-sizes in the range 0.02–2000 µm. Standard reference materials with mean diameters of 32 and 125 µm were used to monitor accuracy, while three repeat runs for each sample were used to monitor precision (reported at < 0.5% SD). The particle distribution output was then processed using the Gradistat software for sediment parameters (Blott and Pye 2001).

Multi-Sensor Core Logger Data

Gamma density values for JC060-21 were measured using the *Geotek* MSCL-S (Standard Multi-Sensor Core Logger). The measurement interval was 1 cm. Magnetic susceptibility was measured using a Bartington Instruments point sensor fitted to a Geotek MSCL-XYZ logger at 0.5 cm down core resolution.

Water Content

Samples were obtained at 5 cm intervals. To obtain volumetric sub-samples of 6.8 cm^3, cubes were pushed into the split sediment core surface. These fresh wet sediment samples of known volume were weighed. The same volumetric samples were then dried at 40 °C for 48 h to a constant weight. The water content wt.% was calculated as the difference between wet weight and dry weight relative to the original wet weight.

Results

Correlation of Itrax-Scan Data with Conventional WD-XRF

Measured concentration data values obtained from conventional WD-XRF and the Itrax-scan data for core JC060-021-PC05 are plotted in Fig. 6.3. The WD-XRF data were measured on 1 cm subsamples; the Itrax data presented are the mean values of scan data for the depth corresponding to the subsample. The elements show highly variable responses. For instance, K, Ti, Fe, Mn, V, Ni, Zn, Ba, Sr and Zr yield strong positive relationships, in a linear form. Ca showed a generally positive but highly scattered relationship that was not statistically significant. Si showed a highly scattered, non linear relationship.

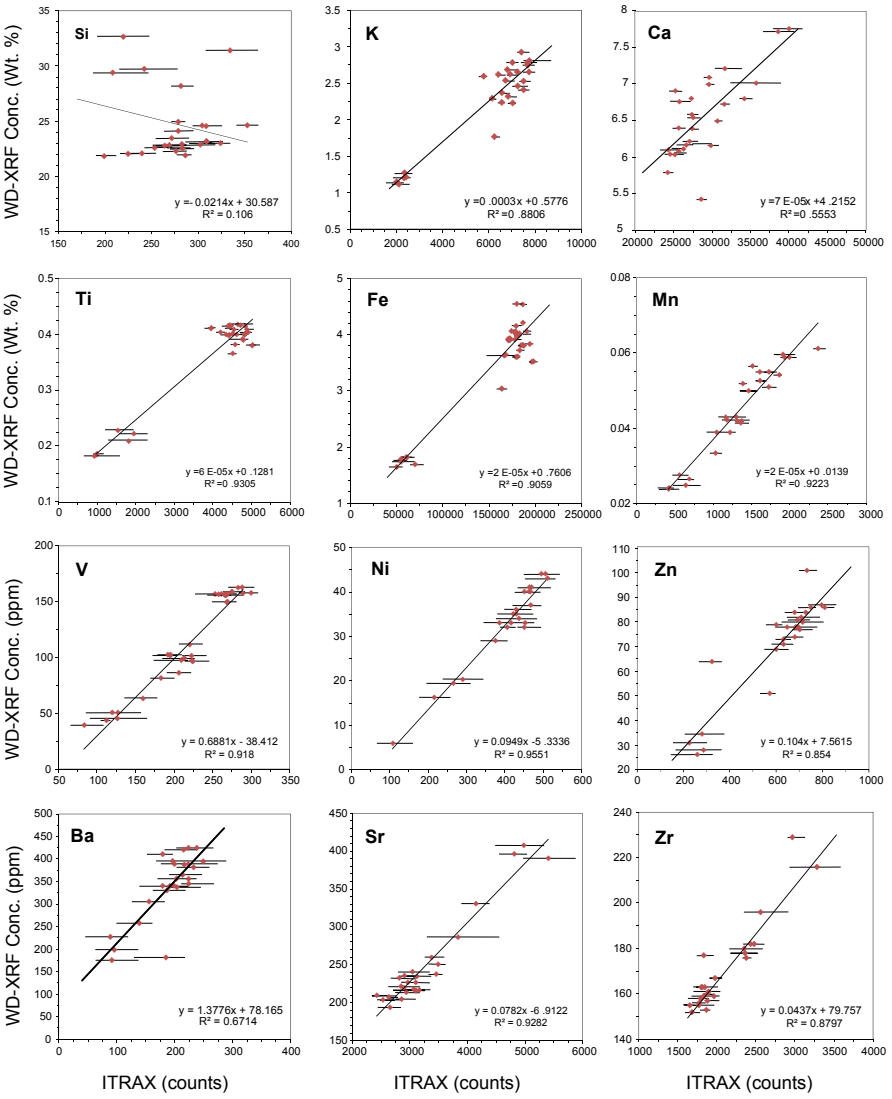

Fig. 6.3 Correlations of Itrax element counts (counts per second) with conventional WD-XRF concentrations. Note: WD-XRF measurements were made on a 1 cm thick slice at each selected depth. The Itrax scan was undertaken at 1 mm step size; the *range bar* indicates the data spread across the 1 cm thickness that corresponds to the WD-XRF measurement. The *point* indicates the average value across the range

Correlation of Water Content Adjusted Itrax-Scan Data with Conventional WD-XRF

To consider the potential effect of the variable water content on Itrax-scan data, we considered water content at each of the sample depths. Water corrected element

Table 6.1 Correlation coefficients (R^2) for linear regression of XRF-scan to respective WD-XRF value and water content corrected XRF-scan to respective WD-XRF

Element	R^2 value XRF-scan	R^2 value Water corrected XRF-scan
Si	0.106	0.4663[a]
K	0.8806	0.7576
Ca	0.5553	0.4785
Ti	0.9305	0.8194
Fe	0.9059	0.8047
Mn	0.9223	0.8465
V	0.918	0.7922
Ni	0.9551	0.823
Zn	0.854	0.8313
Ba	0.6714	0.5288
Sr	0.9282	0.9406[a]
Zr	0.8797	0.9004[a]

[a] Element R^2 improved by water correction

integrals (I_{corr}, based on the measured percentage water content, W, and Itrax wet integrals, I_{wet}, assuming a linear relationship, using Eq. 6.1) were calculated to investigate the potential water content effect.

$$I_{corr} = \frac{I_{wet}(100 - W)}{100}. \tag{6.1}$$

Table 6.1 indicates that the water correction only improves the relationship for Si, Zr and Sr. The Si still shows a highly scattered relationship that is not statistically significant. For all other elements (K, Ca, Ti, Fe, Mn, V, Ni, Zn, Ba) the relationship is weakened and statistically less robust.

Discussion

The observed Itrax scan data deviations from the 'reference' data (WD-XRF) are attributed to the influence of physical properties during the scanning process. The deviations have a more significant effect on the relatively light elements (Si and Ca, see Fig. 6.3). It is likely that the deviations are primarily due to variability in water content, grain-size and sediment heterogeneity (Figs. 6.4 and 6.5).

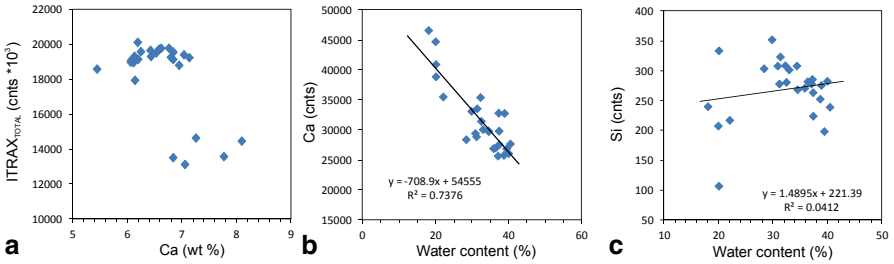

Fig. 6.4 Effects observed in the Itrax Ca and Si intensity data: **a** correlation between total intensity and WD-XRF Ca (wt.%); **b** correlation between Itrax Ca intensity (counts) and water content (%); **c** correlation between Itrax Si intensity (counts) and water content

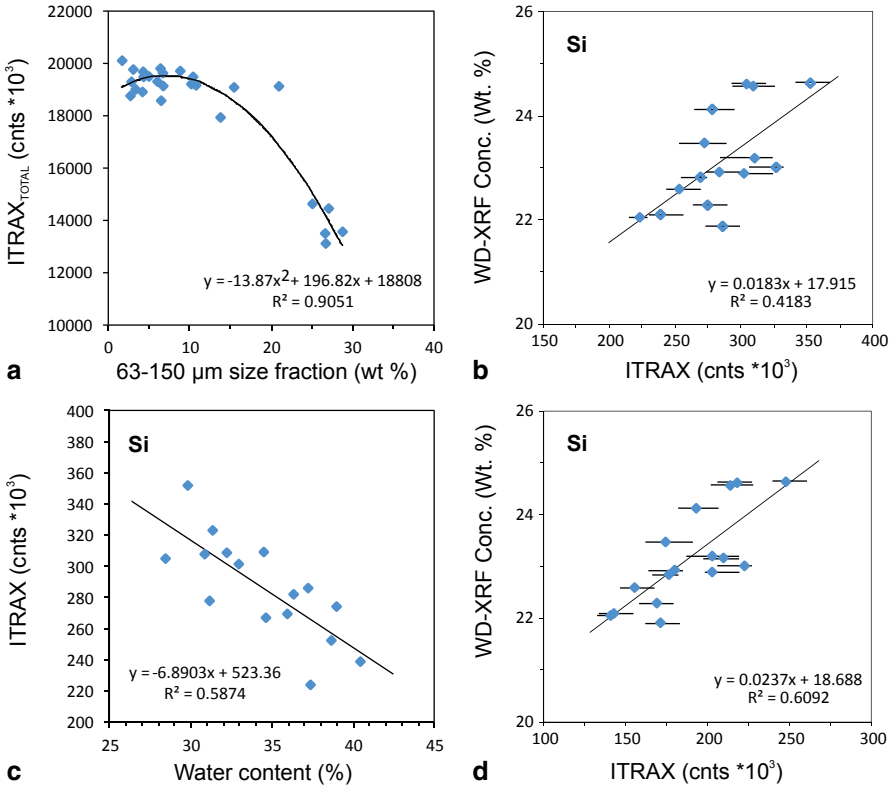

Fig. 6.5 Effects observed due to grain-size variations down core: **a** correlation between total Itrax intensity and 63–150 µm grain-size fraction (wt.%); **b** correlation between WD-XRF Si (wt.%) and Itrax Si intensity (counts) with exclusion of the coarse grained samples (i.e. plotting only clay dominated samples; **c** correlation between Itrax Si intensity (counts) and water content (%) with exclusion of the coarse grained samples; **d** correlation between WD-XRF Si (wt.%) and water content corrected Itrax Si intensity (counts) with the exclusion of the coarse grained samples

Water Effects

Tjallingii et al. (2007) showed that variability in calcium carbonate ($CaCO_3$) content down core may have a greater influence on the total intensity recorded by the Avaatech XRF scanner than changes in wet bulk density and grain-size. This was established for a marine sediment core with a range of $CaCO_3$ concentrations from ~30 to 60 wt.%. WD-XRF analysis for core JC060-021-PC05 indicates the Ca content to be much lower, typically around 6–7 wt.%. Figure 6.4a shows that at relatively low and stable Ca content that there is no effect on the total intensity recorded. The drop in total intensity that is observed for five data points is likely to be a result of sediment type, as these samples were from the coarse grained sections of the core. Figure 6.4b indicates that there is a correlation between Ca intensity and water content; clearly showing high Ca count rates for samples with low water content (~20–25 %) compared with 50–100 % lower count rate when the water content increases to 35–40 % range. This is not statistically robust although shows a similar trend to the relationship observed by Tjallingii et al. (2007). Other factors influencing the Ca intensity in core JC060-021-PC05 may be related to the dominant clay matrix. It is postulated that underestimation of Ca concentrations (by XRF scanners) where foraminifera are abundant is a result of the artificial burial of carbonate tests into the clay matrix during surface smoothing of the split core surface (Kido et al. 2006). Preparation of the split core surface for XRF scanning may decrease the volume of foraminifera in the upper several tenths/hundredths of a micron of the analysed sediment (Richter et al. 2006). However, Hunt et al. (2015, this volume) report that the Itrax data is robust for Ca concentrations above 15 wt.% (with a recorded R^2 value of 0.96). This suggests there may be a concentration threshold to achieve quality Ca data using the Itrax core scanner. We postulate that this threshold is between 8.5 and 15 wt.% Ca concentration, above 15 wt.% Ca the data quality is significantly improved.

The study by Tjallingii et al. (2007) similarly shows a relationship between Si intensity and water content. Figure 6.4c shows that the Si intensity/water content relationship is weak for core JC060-021-PC05. This demonstrates it is very difficult to isolate the dominant contributing factor influencing XRF core scanner elemental data, and it may be a combination of effects that produces poor data quality for the lighter elements such as Si.

Grain-Size and Surface Roughness

Deep sea sediments are predominantly fine grained sediments consisting of clays and silts with little material coarser than >63 μm. Core JC060-021-PC05 predominantly consists of a glaciogenic mud sequence with sparse coarse-grained horizons, capped with a thin (<20 cm) surface layer of coarser, sandy sediment (Fig. 6.2). It therefore seems likely that grain-size is of minor influence across the majority of Itrax-scanned elemental data. However, the top section of the core JC060-021-PC05 contains up to 85 wt.% coarse grained material (>63 μm); consequently, some

grain-size effects are observed in the data (e.g. for total intensity, Figs. 6.2 and 6.5a). Surface roughness effects are more pronounced in sediments dominated by coarser sand-sized grains (Richter et al. 2006). For example, Fig. 6.5a shows that there may be a threshold to the amount of coarse grains within a sample before there is a significant effect on the total intensity. The data suggest that the threshold occurs between 20 and 25 wt.% of grains >63 μm size.

A minor grain-size effect is observed in the Si data, when the data for the clay-dominated samples are plotted the relationship between the conventional WD-XRF and the Itrax-scan counts is observed (Fig. 6.5b). The R^2 value was previously 0.106 (Fig. 6.3), but when the sand dominated data point is removed the R^2 value is 0.4183, suggesting that the Si data may be affected by grain-size and roughness, more evident when the sediment coarse fraction reaches a threshold of >25 wt.%. This finding is supported by Bertrand et al. (2015, this volume) who also confirm that Itrax data quality are influenced where sediment cores show large grain-size variations. Figure 6.5c indicates that the fine sediment Si samples (dominated by <63 μm fraction) shows a weak correlation with water content suggesting that there is both a water content and grain-size effect within the Si data. This demonstrated in Fig. 6.5d by plotting the water corrected Si data for only the fine grained samples. The R^2 value for the uncorrected data was 0.106 compared with the corrected value of 0.6092. It is noted that this is still a weak correlation, however, it demonstrates the complex relationship of the physical properties that can affect the data quality especially for the lighter elements.

Conclusions

A review of previous investigations and the findings of this study suggest that the Itrax and Avaatech XRF core scanners are similarly affected by split core sediment heterogeneity. The Itrax-scan data from a marine sediment core illustrate how the data quality can be affected by physical and chemical properties at the split core surface. It is therefore, important to consider the impact of water content and grain size before making substantive palaeoenvironmental interpretations. For instance, increases in grain-size (>63 μm) and water content may substantially affect data quality in small sections of the core potentially; e.g. turbidite sands leading to misinterpretation of proxies.

References

Bertrand S, Hughen K, Giosan L (2015) Limited influence of sediment grain size on elemental XRF core scanner measurements. This volume

Blott SJ, Pye K (2001) Gradistat: a grain-size distribution and statistics package for the analysis of unconsolidated sediments. Earth Surf Proc Land 26:1237–1248

Croudace IW, Rindby A, Rothwell RG (2006) ITRAX: description and evaluation of a new multi-function X-ray core scanner. In: Rothwell RG (ed) New techniques in sediment core analysis, vol 267. Geological Society Special Publication, London pp 51–63

Croudace IW, Romano E, Ausili A, Bergamin L, Rothwell RG (2015) X-ray core scanners as an environmental forensic tool: a case study of polluted harbour sediment (Augusta Bay, Sicily). This volume

Guyard H, Chapron E, St-Onge G, Anselmetti FS, Arnaud F, Magand O, Francus P, Mélières M-A (2007) High-altitude varve records of abrupt environmental changes and mining activities over the last 4000 years in the Western French Alps (Lake Bramant, Grandes Rousses Massif). Quat Sci Rev 26:2644–2660

Hennekam R, de Lange G (2012) X-ray fluorescence core scanning of wet marine sediments: methods to improve quality and reproducibility of high-resolution paleoenvironmental records. Limnol Oceanogr Meth 10:91–1003

Howe JA (1995) Sedimentary processes and variations in slope-current activity during the last glacial-interglacial episode on the Hebrides Slope, northern Rockall Trough, North Atlantic ocean. Sediment Geol 96:201–230

Howe JA (1996) Turbidite and contourite sediment waves in the Northern Rockall Trough, North Atlantic ocean. Sedimentology 43:219–234

Hunt JE, Wynn RB, Talling PJ, Masson DG (2013) Frequency and timing of landslide-triggered turbidity currents within the Agadir Basin, offshore NW Africa: are there associations with climate change and slope sedimentation rates? Mar Geol 346:274–291

Hunt JE, Croudace IW, MacLachlan SE (2015) Use of calibrated Itrax XRF data in examining turbidite composition and provenance in Agadir Basin, Northwest African Passive margin. This volume

Kenyon NH (1986) Evidence from bedforms for a strong poleward current along the upper continental slope of Northwest Europe. Mar Geol 72:187–198

Kido Y, Koshikawa T, Tada R (2006) Rapid and quantitative major element analysis method for wet fine-grained sediments using an XRF microscanner. Mar Geol 229: 209–225

Masson DG Howe JA, Stoker MS (2002) Bottom current sediment waves, sediment drift and contourites in the northern Rockall Trough. Mar Geol 192:215–237

Masson DG, Bett BJ, Billet DSM, Jacobs CL, Wheeler AJ, Wynn RB (2003) The origin of deep-water, coral-topped mounds in the northern Rockall Trough, Northeast Atlantic. Mar Geol 194:159–180

Richter RO, van der Gaast S, Koster R, Vaars A, Gieles R, de Stigter HC, de Haas H, van Weering TCE (2006) The Avaatech XRF Core Scanner: technical description and applications to NE Atlantic sediments. In: Rothwell RG (ed) New techniques in sediment core analysis, vol 267. Geological Society Special Publication, London pp 39–50

Rothwell RG, Rack FR (2006) New techniques in sediment core analysis: an introduction. In: Rothwell RG (ed) New techniques in sediment core analysis, vol 267. Geological Society Special Publication, London pp 1–29

Rothwell RG, Hoogakker B, Thomson J, Croudace IW, Frenz M (2006) Turbidite emplacement on the southern Baleraic Abyssal Plain (western Mediterranean Sea) during Marine Isotope Stages 1–3: an application of ITRAX XRF scanning of sediment cores to lithostratigraphic analysis. In: Rothwell RG (ed) New techniques in sediment core analysis, vol 267. Geological Society Special Publication, pp 79–98

Ryan WBF, Carbotte SM, Coplan JO, O'Hara S, Melkonian A, Arko R, Weissel RA, Ferrini V, Goodwillie A, Nitsche F, Bonczkowski J, Zemsky R (2009) Global multi-resolution topography synthesis. Geochem Geophys Geosyst 10:Q03014. doi:10.1029/2008GC002332

Serpetti N, Gontikaki E, Narayanaswamy BE, Witte U (2013) Macrofaunal community inside and outside of the Darwin Mounds special area of conservation, NE Atlantic. Biogeosciences 10:3705–3714

Stoker MS, Akhurst MC, Howe JA, Stow DAV (1998) Sediment drifts and contourites on the continental margin off northwest Britain. Sediment Geol 155:33–51

Tian J, Xie X, Ma W, Jin H, Wang P (2011) X-ray fluorescence core scanning records of chemical weathering and monsoon evolution over the past 5 Myr in the southern South China Sea. Paleoceanography:PA4202. doi:10.1029/PA002045

Tjallingii R, Röhl U, Kölling M, Bickert T (2007) Influence of the water content on X-ray fluorescence core-scanning measurements in soft marine sediments. Geochem Geophys Geosyst Geosy Geosyst 8:Q02004. doi:10.1029/2006GC001393

Westerhold T, Röhl U, Laskar, J, Raffi I, Bowles J, Lourens LJ, Zachos JC (2007) On the duration of magnetochrons C54r and C25n and the timing of early Eocene global warming events: implications from the Ocean Drilling Program Leg 208 Walvis Ridge depth transect. Paleoceanography:PA2201. doi:10.1029/2006PA001322

Wilhelms-Dick D, Westerhold T, Röhl U (2012) A comparison of mm scale resolution techniques for element analysis in sediment cores. J Anal At Spectrom 27:1574–1584

Ziegler M, Simon MH, Hall IR, Barker S, Stringer C, Zahn R (2013) Development of Middle Stone Age innovation linked to rapid climate change. Nature Commun 4:1905. doi:10.1038/ncomms2897